ISSN 0869-5911, Petrology, 2021, Vol. 29, No. 6, pp. 597–613. © Pleiades Publishing, Ltd., 2021.
Russian Text © The Author(s), 2021, published in Petrologiya, 2021, Vol. 29, No. 6, pp. 569–587.

Sulfur Isotope Composition of Olivine Gabbronorites from a Mineralized Apophysis of the Yoko-Dovyren Intrusion, Northern Transbaikalia, Russia

A. A. Ariskin[a, b, *], I. V. Pshenitsyn[a, b], E. O. Dubinina[c], S. A. Kossova[c], and S. N. Sobolev[a, b]

[a] *Faculty of Geology, Moscow State University, Moscow, Russia*

[b] *Vernadsky Institute of Geochemistry and Analytical Chemistry, Russian Academy of Sciences, Moscow, Russia*

[c] *Institute of Geology of Ore Deposits, Petrography, Mineralogy and Geochemistry, Russian Academy of Sciences, Moscow, Russia*

**e-mail: ariskin@rambler.ru*

Received March 29, 2021; revised April 28, 2021; accepted May 5, 2021

Abstract—High-precision analysis of sulfur isotope composition was carried out for sulfide fractions from ten samples of olivine gabbronorite that composes a thick (approximately 300 m) swell of a ore-bearing apophysis that is parallel to the basal part of the Yoko-Dovyren massif in northern Baikal area, Russia. The $\delta^{34}S$ values were found out to widely vary from +11‰ to –1.9‰. The maximum enrichment in isotopically heavy sulfur was identified within the basal horizon, which is 10 m thick, whereas the minimum values of $\delta^{34}S$ were observed near the upper contact of the intrusive body. Sulfide droplets in chilled picrodolerite from the lower contact zone (Pshenitsyn et al., 2020) show a narrow range of $\delta^{34}S$ (+8.65 ± 0.34‰, $n = 5$). Lower values of $\delta^{34}S$ ranging from +2.09 to +2.53‰ are characteristic of the sulfide-rich net-textured ores, the mineralized olivine gabbronorite, and a cutting leucogabbro dike. The sulfur isotope compositions of two samples of pyrite-bearing rocks from the host carbonate–terrigenous rocks display discrete values of $\delta^{34}S = +2.20$‰ and $\delta^{34}S = +9.40 \pm 0.14$‰ at a whole-rock sulfur concentration up to 3.5 wt %. Simple scenarios of the additive mixing of isotope-contrasting reservoirs corresponding to a juvenile magmatic source ($\delta^{34}S = 0$ and +2‰) and a provisionally chosen contaminant ($\delta^{34}S = +9.4$‰) are demonstrated to require a high degree of assimilation of host rocks (as much as 60–80%) and complete isotope equilibration of the hybrid system. In the contact picrodolerite with rare globular sulfides, the mixing mechanism is inconsistent with the estimated sulfur solubility in its parental magma: approximately 0.08 wt % (Ariskin et al., 2016). The high $\delta^{34}S$ values in rocks from the basal part of the apophysis may be explained, under the assumption that contact-metamorphic H_2S-bearing fluid was introduced into the magmatic system, by the thermal decomposition of pyrite coupled with dehydration of the host rocks. The proposed mechanism does not require a volume assimilation of crustal materials and is consistent with petrological and geochemical characteristics of the Dovyren magmas and derivative cumulates.

Keywords: Yoko-Dovyren massif, apophysis, sulfide ores, plagioperidotite, sulfur isotope composition, contamination, pyrite decomposition, fluid-assisted material transfer

DOI: 10.1134/S0869591121060023

INTRODUCTION

The origin of Cu–Ni–PGE sulfide mineralization in layered intrusions involves mechanisms responsible for the localization of sulfide accumulations and the formation of orebodies, which depend on the parameters of silicate–sulfide liquid immiscibility as a factor controlling the origin of protosulfide liquids (Naldrett, 2004, 2011). It is therewith assumed that the base metals (Fe–Ni–Cu–Co) and PGE are provided by the magmas themselves, from which these elements are extracted into the sulfide phase. This subdivision into the *dynamic* (transport phenomena) and *physicochemical* (*P–T* parameters, magma compositions, etc.) aspects of the ore-forming processes implies that the dynamics of magma emplacement in a specified geological–tectonic environment is interrelated with the migration of immiscible sulfides through the crystallizing magmas and cumulates (Rad'ko, 1991, 2016; Maier, 2001, 2005; Likhachev, 2006; Song et al., 2011; Chung and Mungall, 2009; Barnes et al., 2016; Robertson et al., 2016; Mao et al., 2018; Wang et al., 2020; Yao and Mungall, 2021). In both instances, it is critically important to estimate timing of the silicate–sulfide liquid immiscibility, i.e., to understand which factors controlled the relatively early or late origin of the very first sulfide globules in the magmas. The dominant factors are the decrease in the sulfur concentration at sulfide saturation (SCSS)

during the fractionation of mafic–ultramafic magmas and the probability of crustal contamination, which involves the effects of decreasing SCSS when the magma interacts with more felsic rocks and/or sulfur introduction into the magma systems from the host rocks. Starting from the 1960s, the "factor of sulfur introduction" is thought to control the origin and accumulation of sulfides in magmatic systems, regardless of the types and resources of the corresponding Cu–Ni–PGE deposits (Naldrett, 2004, 2011). It is pertinent to mention that proponents of this viewpoint ceased to be so categorical over the past few decades.

On the one hand, experience gained in the experimental modeling and thermodynamic simulations of SCSS (Li and Ripley, 2009; Baker and Moretti, 2011; Ariskin et al., 2013, 2018a; Fortin et al., 2015; Kiseeva and Wood, 2015) indicates that the effect of felsic contaminants on SCSS is insignificant. On the other hand, data on various mineralized volcano-plutonic complexes imply that additional sulfur introduction into the magma conduits and chambers is not necessary for sulfide liquid immiscibility to emerge, and the juvenile sulfur concentrations are commonly sufficient for magma saturation with respect to protosulfide liquids already after 20–30% silicate crystallization (Maier and Groves, 2011; Ariskin et al., 2016, 2018a, 2018b). This led to the viewpoint that the introduction of crustal sulfur into orthomagmatic systems predetermines the origin of supergiant and other economically important Cu–Ni sulfide deposits, whereas smaller occurrences of ore mineralization and sulfide orebodies might have been formed in the basal portions of magma chambers and in the feeders as a consequence of the crystallization of the parental magmas (Ripley and Li, 2013; Karykovski et al., 2018; Ariskin et al., 2018). Some researchers believe that crustal contamination cannot play any significant role even in producing giant deposits (Krivolutskaya, 2016).

This situation implies that sulfides in individual intrusive complexes may have been formed under broadly varying conditions so that solutions of genetic problems are to be predetermined by the possibility of computation of SCSS trajectories in the course of crystallization of primary and contaminated mafic–ultramafic magmas (including the application of contamination criteria for estimating the scales of the processes). This paper is devoted to the analysis of these problems with reference to plagioperidotites of the Baikal Cu–Ni sulfide deposit in the northern Baikal area. The problems are attacked with the application of newly acquired data on the isotope composition of the sulfides.

ORE POTENTIAL OF THE DOVYREN INTRUSIVE COMPLEX

The **Baikal deposit** was discovered based on results of exploration operations conducted at the Yoko-Dovyren massif by the Baikal Multipurpose Geological Team of the North Baikal Expedition in 1963–1964 under supervision of L.M. Baburin (Baburin, 1964). This large layered intrusion occurs at a distance of approximately 60 km of Lake Baikal and is topographically expressed as a long ridge (Dovyren Ridge), which is the watershed between the Tyya, Ondoko, and Olokit rivers and trends 45°–50° northeastward. The Ondoko River cuts across intrusive rocks in the southwestern flank of the body, where its closure part is made up of rocks analogous to those composing the lower nearby ridge of Yoko. Geological maps show the Yoko-Dovyren massif as a lens-shaped body with steep contacts (dipping at 80°–90°), approximately 26 × 35 km, which is nearly exactly conformable with the host carbonate–terrigenous rocks of the Ondoko Group in the Synnyr rift (Gurulev, 1965; Konnikov, 1986; Kislov, 1998; Rytsk et al., 2002). The intrusive rocks of the Dovyren complex were dated at 724–728 Ma (Ariskin et al., 2013; Ernst et al., 2016).

Geophysical data indicate that the regional area of the Bouguer gravity anomaly is several times larger than the outcropped part of the Yoko-Dovyren massif (Turutanov et al., 2013). Gravimetric data processed with the application of 3D modeling techniques show that the intrusion is now an elongate flattened body (its width is two to three times greater than its maximum stratigraphic thickness), with much of its top portion not exposed at the surface and occurring at depths of 500–1000 m. The intensity of the gravity anomalies suggests that the massif extends northeastward and grades into another body (1–1.5 km thick) at a depth, at a distance of about 10 km from the closure exposed at the surface (Turutanov et al., 2013). It is reasonable to hypothesize that this is an intermediate chamber that connects the main intrusion with flows of low-Ti basaltic andesites that crown the Ondoko Group in a unit of volcano-sedimentary rocks (Manuilova and Zarubin, 1981).

Depending on the assumed difference between the densities of the rocks composing the massif and hosting it, the depths of the bottom of this massif were evaluated at 1.5–2 to 3 km. It should be mentioned that the current setting of the massif calculated from geophysical data does not necessarily correspond to its original setting and stratigraphy. In other words, the gravimetric interpretations of the "top" and "bottom" of the massif are hardly consistent with the positioning of the real contacts of the intrusion because of its overturned vertical stratigraphic sequence. Hence, the isopachs of the buried top of the massif also cover its portions a few kilometers away from its exposed lower and upper contacts. The positive gravity anomalies in the peripheral parts of the main chamber may reflect the occurrence of accompanying gabbronorite dikes and plagioperidotite sills[1].

[1] The term *plagioperidotite* is used herein as a tribute to the traditional geological description, for example, in (Kislov, 1998). In fact, the bodies are made up of olivine gabbronorite with a broadly varying olivine content (Ariskin et al., 2018) and are usually cut across by leucocratic gabbronorite dikes. These variations are more adequately reflected by the term *gabbro–peridotite sills* (Orsoev et al., 2018).

The **high-grade ores of the Baikal deposit** occur off the main intrusion, in sills that are situated beneath it and are connected with its hyperbasite basal portion in its central part (Kislov, 1998; Orsoev et al., 2018; Pshenitsyn et al., 2020, 2022). These observations are consistent with the conclusions that the sulfides were localized in intermediate chambers and branches of the magma conduits (see above) and are based on data on four thoroughly studied areas with ore mineralization: Ozernyi (in the northeastern termination of Dovyren), Tsentralnyi and Bolshoi (named after streams and rivers flowing across the thickest central part of the body), and Rybachii (southwestern termination) (Baburin, 1964). Later exploration operations at the Yoko-Dovyren massif were not as intense (A.G. Krapivin in 1976–1979 and V.V. Kletkin in 1986–1990). After follow-up exploration operations headed by A.G. Stepin in 1989–1993, the predicted resources of the Baikal deposit were evaluated at 147 kt of Ni, 51.01 kt of Cu, and 9.47 kt of Co (Kislov and Khudyakova, 2020), and the deposit was ascribed to the off-balance (uneconomic) category.

Nevertheless, ore-forming processes at the Dovyren complexes stimulated continuous interest of many researchers. Over the past years, many scientists (A.A. Ariskin, E.V. Kislov, D.A. Orsoev, I.V. Pshenitsyn, and E.M. Spiridonov) continued to focus attention on the sulfide-bearing rocks and ores of this unique massif. This is largely explained by the broad variability of the Cu–Ni–PGE sulfide mineralization, the distribution patterns of aureoles of disseminated mineralization near the sulfide ores, and the discovery of new areas with PGE mineralization (Ariskin et al., 2020). The recent studies used newly developed techniques, including the simulation of crystallization of sulfide magmas and applied aspects of X-ray computed tomography, CT (Ariskin et al., 2016, 2018a, 2018b, 2018c; Korost et al., 2019). It is particularly interesting to study rocks hosting sulfide globules, which were found near the lower contacts of the mineralized sills/apophyses and suggest that the immiscible sulfide liquids were formed in the chambers, and this took place before their segregation and the development of large accumulations (Pshenitsyn et al., 2020). The latter paper presents CT data on sulfide globules and irregularly-shaped blebs, up to net-textured ores, and estimates of the composition of the protosulfide melts, which were done to identify possible correlations between the textural–mineralogical types of the mineralized rocks and their isotopic–geochemical characteristics.

EARLIER DATA ON THE SULFUR ISOTOPE COMPOSITION

The very first estimates of the sulfur isotope ratios of sulfide-bearing rocks from an occurrence of ore mineralization at Dovyren were made in the mid-1960s, when ten representative samples of pyrrhotite yielded $-0.6 \le \delta^{34}S \le +3.4‰$, $+1.8‰$ on average (Vinogradov and Grinenko, 1964). These measurements were carried out on one of the Soviet Union's first mass spectrometers MS-2M (manufactured in 1953), with more advanced mass spectrometric tools subsequently manufactured by this plant in the town of Sumy: MI1201 (1969–1971) and MI1305 (Izrailevich et al., 2003). The equipment was invented when a method for sulfur extraction in the form of SO_2 was developed at the Vernadsky Institute in Moscow. The procedure was conducted by means of stepwise heating of powdered samples and V_2O_5 in a vacuum-pumping assembly and the subsequent removal of CO_2 and H_2O from the gas mixture. These methods were shortly afterward adopted at many research institutions of the former Soviet Union. For example, these were data on the sulfur isotope composition of pyrrhotite from seven mineralized-plagioperidotite samples from the Yoko-Dovyren massif reported in (Gurulev et al., 1978), which lied within a narrower range of $-0.5 \le \delta^{34}S \le +1.05‰$, $+0.3 \pm 0.5‰$ on average (analyst M.Sh. Koviladze, Georgian Republican Center for Isotope Studies in Tbilisi, Georgia, Soviet Union). Data in (Grinenko, 1986) characterize 34 samples of rocks with poor mineralization from the upper and lower inner-contact zones of this intrusion. Sulfur concentrations in two-thirds of the samples were no higher than 0.01 wt % and were no higher than 0.3 wt % in the rest. The near-roof and chilled rocks from the lower contact zone show significant variations in their $\delta^{34}S$, from -3.8 to $+14.9‰$, whereas the compositions of most samples of rocks of the layered series fall within a narrower range of $+0.2$ to $+4‰$, $3.3 \pm 0.7‰$ on average (Grinenko, 1986).

A representative data set acquired at about the same time at the same laboratory in Tbilisi characterized 45 fractions of pyrrhotite and sphalerite in one of the samples from the ore mineralization of different type (Kacharovskaya et al., 1986). The newly collected samples of the mineralized plagioperidotites yielded lower $\delta^{34}S$ values ($+0.12‰$ on average), whereas the gabbronorites with disseminated sulfides showed a tendency toward depletion in the heavy ^{34}S isotope ($\delta^{34}S = -0.38 \pm 0.95‰$). The average values for the massive and breccia ores are $+0.89 \pm 1.32‰$ and $+1.22 \pm 0.78‰$, respectively. Later on samples from Dovyren were studied at the Laboratory for Isotope Studies and Geochronology of the United Institute of Geology and Mineralogy, Siberian Branch, Russian Academy of Sciences, in Novosibirsk on a Finnigan (modification D) mass spectrometer (Glotov et al., 1998). The study was conducted with 44 whole-rock sulfide samples from the dominant types of the mineralized plagioperidotites, massive and disseminated ores, and (mostly) sulfide-bearing gabbroic rocks and anorthosites from two platiniferous reefs of the Yoko-Dovyren massif (Distler and Stepin, 1993; Kislov, 1998) at the Ozernyi, Tsentralnyi, Bolshoi, and Ryba-

chii prospects. In addition, analyses were made for several samples of the host rocks, a pyrite-bearing quartz vein, and a galena–barite veinlet from the Rybachii Prospect.

Figure 2 shows some of the 1964–1998 results: data on the high-grade ores containing more than 5% sulfides (n = 32) and related sulfide-bearing plagioperidotites (n = 15) from the basal part of the massif. These data demonstrate that the sulfur isotope composition becomes insignificantly but systematically heavier in the ore samples. No data are available on the possible spatial variations in $\delta^{34}S$ in the areas, particularly in relation to the position of the sampling sites relative to contacts with the host rocks or in the vertical sections of the mineralized sills/apophyses. Data published herein partly bridge this gap with reference to the widely known mineralized body below the contact between the Yoko-Dovyren massif; this body consists of several of types of ores and sulfide mineralization: apophysis DV10 (Pshenitsyn et al., 2022).

SAMPLES

According to results of exploration operations in 1964–1979, high-grade breccia (locally net-textured) ores were found below the bottom of the Yoko-Dovyren massif in the area of Bolshoi Stream. The ores were constrained to the holocrystalline rocks of an unnamed plagioperidotite sill. According to mapping data acquired by A.G. Krapivin and A.G. Stepin (see above), this sill connects with the basal zone of the pluton in the watershed area of Bolshoi and Tsentralnyi streams (northeastern occurrence of ore mineralization) and is, in fact, an apophyse (a long branch), which is mostly parallel to the general strike of the structure (Fig. 1). According to (Konnikov, 1986), the orebody is constrained to the central part of this body, and its "...marginal chill picrite zone is devoid of ore mineralization...". In 2006–2019, we traced the upper and lower contacts of the apophysis and thoroughly sampled its rocks, using mostly exploration pits and trenches directed across the body trend. The body itself was then named *apophysis DV10* after the starting point and coordinates of the first profile sampled in 2006. The results of the work show that outcrops of the high-grade ores coincide with a swell of the apophysis (in which its thickness increases to 280 m; the thickness decreases to approximately 150 m southwestward, in the area of Magnitnyi Stream). The sampling procedure, the inner structure of apophysis DV10, and its sulfide mineralization are described in detail in (Pshenitsyn et al., 2022). This material was used in further isotopic–geochemical studies: Table 1 lists the ten samples whose sulfur isotope composition has been studied, along with the stratigraphic setting and major features.

The major-component composition of five rocks from Table 1 is listed in (Pshenitsyn et al., 2022), and that of the other studied samples is presented in Table 2. Figure 3 shows the variations in the normative mineralogical composition of the rocks, which were calculated for all of the analyzed samples. These data indicate that practically the whole vertical section is made up of olivine gabbronorite, and only the lower contact zone includes a thin (approximately 5 m) unit, whose rocks can be classed with picrodolerite and transition varieties based on their textural features. The picrodolerite of the chill contact zone is a massive porphyritic rock with an ophitic groundmass. The rock contains less than 15% large (up to 1.5 mm) olivine phenocrysts, and the ophitic groundmass abounds in small laths of andesine and labradorite and in elongate augite and hypersthene crystals. The minor minerals are phlogopite (about 2.5%) and locally occurring sulfides. The accessory minerals are ilmenite (~1%) and aluminochromite (~0.5%). Olivine content increases upsection, and the primary porosity of the olivine cumulates decreases, as is evident from that the rocks are gradually depleted in incompatible elements, whereas the MgO/Zr ratio increases (Table 1). The grain size of the intercumulus phases also increases, and the rocks become poikilitic owing to plagioclase and pyroxene oikocrysts that cement the variably sized olivine grains with Al-chromite inclusions.

The vertical section thus displays an upward enrichment of the gabbronorite in olivine. Its maximum content of about 70% was found at the stratigraphic levels of 160–190 m (Fig. 3). This tendency is disturbed in the high-grade net-textured ores and dikes of olivine-bearing and/or olivine-free gabbronorite that locally cut portions of the stratigraphic profile of the apophysis. Another important observation is that the rocks of the chill and inner-contact zones are not devoid of sulfide mineralization. We found sulfide mineralization within the lower contact zone already in the course of its primary inspection: sample DV10-4 contains small (1–2 mm) sulfide droplets. Later we found picrodolerite hosting larger roundish sulfide globules ranging from a few to 15 mm near the contact between the body and host black shale (Pshenitsyn et al., 2020).

Sulfide mineralization is seen in all samples from apophysis DV10 and consists of globules (which are commonly irregularly shaped and are as large as 2 mm across) or localized sulfide disseminations, and only the lower part of the body (within 10–20 m from the contact) contains globular and high-grade net-textured ores with about 12 wt % sulfur (or up to ~35% sulfide material, Table 1, Fig. 3). Away from the high-grade ores, the content and size of the net-textured ore material decrease, and the size and content of the blebs also simultaneously decrease. With regard to the textures of the mineralized rocks, they can be classified into four types (Pshenitsyn et al., 2022): (1) inner-contact picrodolerite with sulfide droplets (samples 16DV627-1-2 and 19DV928-1); (2) olivine gabbronorite with sulfide droplets (samples DV10-4 and 16DV627-1-3); (3) mineralized olivine gabbronorite

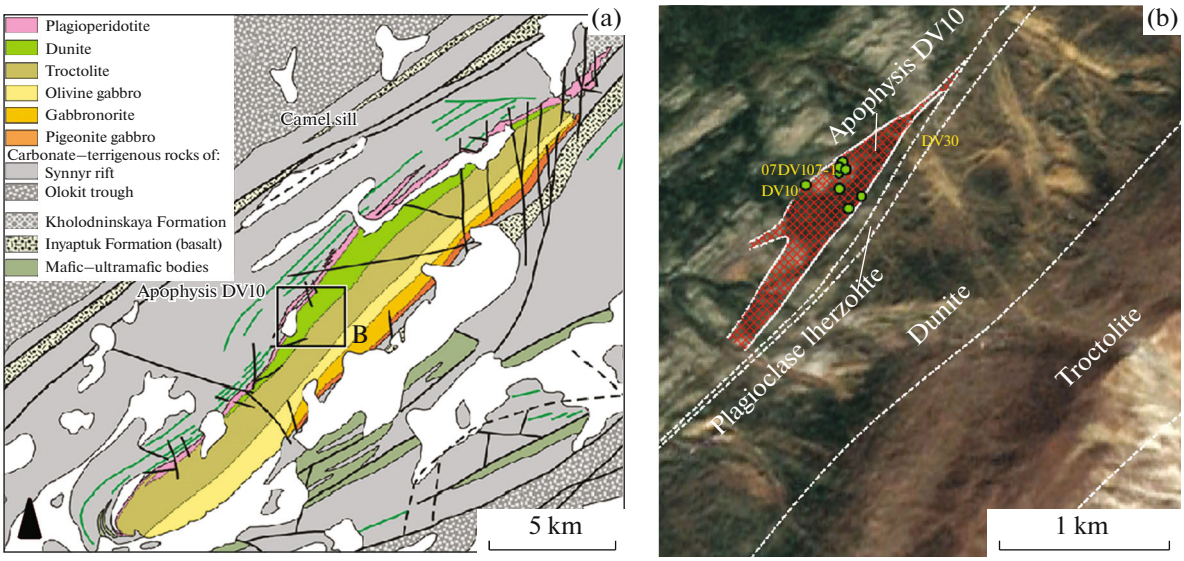

Fig. 1. (a) Geological map of the Yoko-Dovyren massif and (b) the setting of apophysis DV10 and sampling sites (after Pshenitsyn et al., 2020).
Sampling sites are shown only for sulfide-bearing rocks and rocks whose sulfur isotope composition of sulfides was analyzed (Table 1).

with irregularly shaped blebs that grade into domains of net-textured dissemination (sample 16DV628-2); and (4) net-textured ores with a matrix of olivine gabbronorite (sample 07DV107-1) (Table 1, Fig. 4). Sample 16DV629-1-2, which was taken from above the main mineralized horizon, represents a leucogabbro dike with sulfide droplets (Figs. 4c, 4d).

The sulfide mineral assemblages do not correlate with the type of the sulfide mineralization and include pyrrhotite/troilite + pentlandite + chalcopyrite (±cubanite). The minor minerals are sphalerite and galena (Kacharovskaya, 1986). Pyrrhotite and troilite were identified in all of the rocks in the form of typical vermicular lamellas of exsolution *Mss* into pyrrhotite (*Po*) and troilite (*Tr*), which occur in a roughly equal proportions, with rare pentlandite grains. The chalcopyrite (*Cpy*) grains are commonly anhedral and occur in sulfide accumulations and droplets as anhedral grains or aggregates with pyrrhotite. More rarely *Cpy* lamellas are found in a *Po*–*Tr* matrix. Cubanite (*Cub*) was identified as a product of *Iss* exsolution in chalcopyrite, sometimes as elongate lamellas or platelets with scalloped outlines at contacts between pyrrhotite and pentlandite. The pentlandite was found as two varieties: *Pn*-I, which occurs as subhedral aggregates 0.1–0.3 mm usually at pyrrhotite–chalcopyrite contacts, and *Pn*-II, which occurs as flamboyant lamellas in pyrrhotite. It is often constrained to boundaries between sulfide grains and to cracks in sulfide aggregates. Pentlandite lamellas hosted in a single pyrrhotite grain are sometimes parallel. The differences in the composition of the two pentlandite populations are as follows: the composition of *Pn*-I is less variable (31.5–33 wt % Ni), and it contains higher Co concentrations of 1.5 to 2.6 wt %; whereas *Pn*-II is characterized by broader variations in the Ni concentrations (~30–33.5 wt %) and by Co concentrations lower than 1 wt % (Pshenitsyn et al., 2022).

SULFUR ISOTOPE COMPOSITION

The isotope composition of sulfur was studied at the Laboratory of Isotope Geochemistry and Geochronology of the Institute of Geology of Ore Deposits, Petrography, Mineralogy and Geochemistry, Russian Academy of Sciences, in monomineralic sulfide

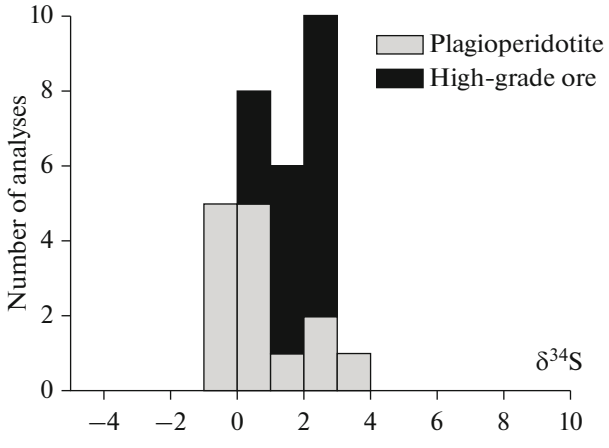

Fig. 2. Histogram of the sulfur isotope composition of the mineralized plagioperidotite and high-grade sulfide ores of the Dovyren intrusive complex (based on results obtained in 1964–1998, review in Kislov et al., 1998, appended in Glotov et al., 1998).

Table 1. Stratigraphic setting and characteristics of the studied rocks of apophysis DV10

Sample	*h*, m	Rock	CIPW, wt %		*Fo* (*Ol*)	MgO	S, wt %	Cu, ppm	$\delta^{34}S$, ‰
			Ol	*Pl*		Zr			
19DV920-1	279.7	Contact picrodolerite	n.d.	n.d.	n.d.	n.d.	n.d.	n.d.	−1.86
19DV903-3	274	Olivine gabbronorite	49.9	28.2	n.d.	5964	0.05	64	1.00
19DV908-1*	190	Olivine gabbronorite	70.2	18.9	83.6	13085	0.63	327	2.42
16DV629-1-2**	23	Mineralized leucogabbro (dike)	n.d.	n.d.	n.d.	n.d.	n.d.	n.d.	2.50 ± 0.17 (n = 3)
16DV628-2*	21	Mineralized Olivine gabbronorite	32.6	23.9	80.6	4157	3.43	824	2.53 ± 0.15 (n = 3)
07DV107-1*	12	Net-textured ore	34.1	8.4	81	18240	9.11	6685	2.09
DV10-4*	11	Olivine gabbronorite **	51.4	20.6	80	5103	0.82	1029	6.20
16DV627-1-3	8	Olivine gabbronorite **	n.d.	n.d.	78.1	5027	0.54	676	10.33 ± 0.42 (n = 3)
19DV928-1	3	Picrodolerite **	n.d.	n.d.	n.d.	2802	0.12	249	11.80
16DV627-1-2 (droplet 1)	0.1	Picrodolerite **	25.5	35.5	75.5	2328	0.22	355	8.76 ± 0.25 (n = 2)
16DV627-1-2 (droplet 2)	0.1	Picrodolerite **	–	–	–	–	–	–	8.48 ± 0.35 (n = 3)

n.d. means than no data are available.
* According to data in Table 1 in (Pshenitsyn et al., 2022). ** Contains sulfide droplets/globules.

fractions. The sulfide material was extracted from polished sections of the samples or immediately from the surface of the samples using a diamond needle. We have studied ten samples. In picrodolerite of sample 16DV627-1-2, two relatively large droplets were studied (Fig. 5). Most of the sulfide samples consisted of pyrrhotite and troilite. From each droplet from sample 16DV627-1-2, we separated single fractions dominated by either chalcopyrite of pentlandite. The portions of the material contained recalculated amount of 30–50 mg pure sulfur, except two portions that contained as little as 8 μg (sample 19DV908-1) and 23 μg (sample 19DV928-1). To conduct isotope analysis, the sulfide mineral samples were converted into SO_2 using a FlashEA HT 1112 element analyzer at 1020°C in a reactor filled with CuO and WO_3. The samples and standards in tin capsules were successively placed into the reactor using an autosampler. The sulfur isotope composition of SO_2 was measured by CF-IRMS in a continuous He flow on a DELTA V + (Finnigan, Germany) mass spectrometer. The internationally certified standards IAEA-S-1 and IAEA-S-2 were measured at the beginning and end of measurements of each series of the samples, and the reference values of the standards (–0.3 and +22.67‰, respectively) were used to calibrate the data on the VCDT (Vienna Canyon Diablo Troilite) scale

$$\delta^{34}S_{sample} = \left(^{34}S/^{32}S\right)_{sample} / \left(^{34}S/^{32}S\right)_{VCDT} - 1.$$

The reproducibility of the data obtained by this technique was ±0.2‰.

The **measurement results** are listed in Table 1 and plotted in Fig. 3. A principal feature seen in the behavior the sulfur isotope system is that the heavy isotope ^{34}S enriches sulfides in the basal part of apophysis DV10 below the main mineralized unit. All of the four samples from the depth range of 0–11 m from the lower contact show $\delta^{34}S$ values from +6 to +12‰, with the maximum enrichment of the ^{34}S isotope typical of the basal picrodolerite with the minimum sulfur concentration (0.12% sulfur or ~0.3% sulfides), whereas the minimum (for this basal unit) value of $\delta^{34}S$ = +6.2‰ was found in the olivine gabbronorite that contains 0.82% sulfur (~2.3% sulfides). Sulfides in the high-grade ores above the unit are not any significantly enriched in the heavy isotope, and their $\delta^{34}S$ varies from +2.1 to +2.5‰. Further upsection, sulfur content in the rocks is only occasionally higher than 0.1 wt %, and the $\delta^{34}S$ values decrease to +1‰ and even to negative values at the upper contact of the apophysis (Fig. 3). The values of $\delta^{34}S$ of five samples from two sulfide globules from picrodolerite at the lower contact (samples 10 and 11 in Table 1) were

Table 2. Chemical composition of the studied rocks from apophysis DV10

Component	19DV921-2*	19DV902-1	19DV903-1	19DV923-1	19DV906-2	19DV910-1	19DV916-1	16DV629-M	16DV629-I	19DV911-2	19DV912-1
	279**	276	274	230	220	30	25	23	23	20	5
Major components, wt %											
SiO_2	44.81	44.04	45.20	45.92	44.13	44.57	44.87	40.22	47.47	40.89	45.78
TiO_2	0.35	0.39	0.42	0.48	0.38	0.42	0.39	0.36	0.43	0.32	0.47
Al_2O_3	7.76	7.65	8.38	9.72	7.87	7.29	7.12	7.63	8.40	6.32	8.76
FeO	11.04	11.65	11.58	12.42	11.69	12.09	12.27	18.34	12.27	11.84	12.90
MnO	0.17	0.18	0.18	0.22	0.18	0.17	0.18	0.17	0.22	0.18	0.19
MgO	25.41	24.82	22.97	20.12	24.12	25.36	25.33	11.51	11.44	27.21	21.58
CaO	5.75	5.56	5.78	7.17	5.70	4.91	5.05	12.08	14.98	4.62	6.38
Na_2O	0.84	0.79	1.06	0.65	1.11	1.12	0.78	1.00	1.45	0.40	1.18
K_2O	0.50	0.48	0.52	0.58	0.67	0.52	0.57	0.33	0.19	0.37	0.69
P_2O_5	0.06	0.08	0.09	0.07	0.07	0.09	0.09	0.05	0.07	0.06	0.08
Cr_2O_3	0.57	0.48	0.45	0.15	0.49	0.50	0.54	0.60	0.33	0.62	0.21
NiO	0.15	0.13	0.12	0.09	0.12	0.12	0.13	0.28	0.08	0.11	0.10
S	0.04	0.03	0.04	0.04	0.04	0.03	0.05	4.19	1.01	0.29	0.12
Total	100	100	100	100	100	100	100	100	100	100	100
LOI	2.54	3.72	3.20	2.36	3.44	2.80	2.63	3.23	1.66	6.78	1.56
Chalcophile elements											
Zn	80	86	78	99	75	83	89	59	62	74	96
Cu	47	28	39	48	36	31	46	1179	1336	176	183

Major components were analyzed by XRF according to the routine NSAM VIMS 439-RS on an Axios mAX Advanced (PANalytical, Netherlands) vacuum spectrometer at the Laboratory for Analysis of Mineral Materials, Institute of Geology of Ore Deposits, Petrography, Mineralogy, and Geochemistry, Russian Academy of Sciences (analyst A.I. Yakushev). For sample 16DV629-1-2, indexes DV629-M and –I pertain to fragments of mineralized leucogabbro, which are poor and relatively rich in chalcopyrite, respectively.
* Sample number. ** Depth, m.

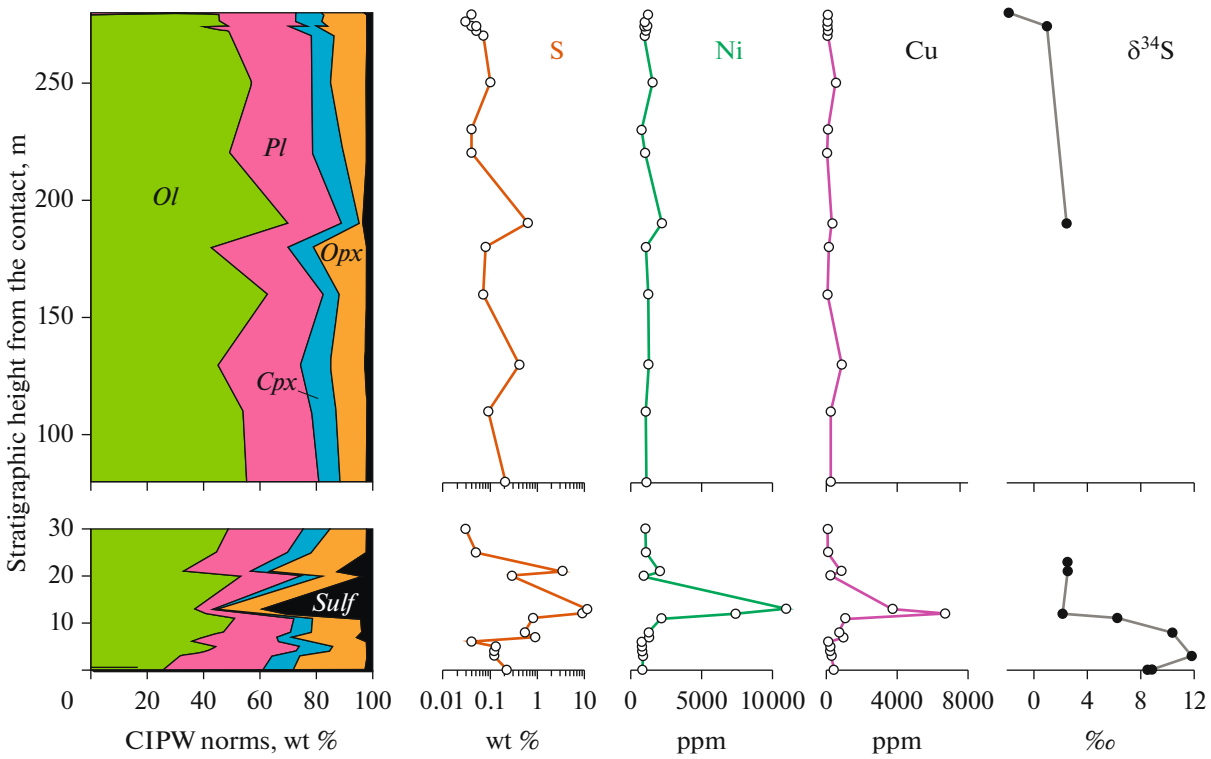

Fig. 3. Variations in the normative composition of the rocks, their sulfur, nickel, and copper concentrations, and their sulfur isotope composition in the stratigraphic section of apophysis DV10.
Based on data form Tables 1 and 2 and on rock analyses in (Pshenitsyn et al., 2022).

undistinguishable within the analytical error: +8.65 ± 0.34‰ (n = 5) on average.

DISCUSSION

The uneven distribution of mineralized rocks in the vertical section of apophysis DV10 indicates that sulfide material was accumulated in the bottom part of the subchamber from the main volume of the gabbronorite magma, which has been saturated with sulfides. The unique setting of the main orebody, which is constrained to a swell of the apophysis, suggests that the vertical transport of sulfides from higher stratigraphic levels (Pshenitsyn et al., 2020) was associated with the horizontal transfer of sulfide masses along the lower contact with host rocks, in the form of heterogeneous magmas or mush of unconsolidated cumulates. These processes were obviously accompanied by the local deposition of sulfides in pockets and potholes (Pshenitsyn et al., 2022). The intercumulus melts were therewith squeezed off the pore space of the subcotectic (*Ol* ± *Pl*) olivine-rich cumulates, as follows from the drastic depletion of the high-grade ores in normative clinopyroxene (see Fig. 3 for the distribution of *Cpx*).

A key problem in the origin of sulfides in the disseminated mineralization and net-textured ores and ore blebs is the source of their sulfur: whether the sulfur was juvenile or it was isotopically heavy sulfur extracted from the host rocks. The answer seems to be self-evident in view of the fact that sulfides in the basal horizon are enriched in isotopically heavy sulfur. However, it is worth mentioning that the highest $\delta^{34}S$ values of approximately +(8–12)‰ are typical of rocks poor in sulfides and occurring near the contact, whereas the sulfur isotope composition of the sulfide ores and sulfides disseminated throughout most of apophysis DV10 is characterized by values no higher than +2.5‰ (Table 1). This limit is consistent with earlier data shown in Fig. 2.

The additive contamination mechanism for the Dovyren magmas shall thus take into account the interaction of the mantle reservoir that had mantle $\delta^{34}S$ values (0 to +2‰) with host rocks, whose sulfur isotope composition varied within broader limits. Of all possible scenarios of the process, the two following ones deserve special mention. According to one of them, the magmas could interact with sulfides in the host rocks, which are enriched in the heavy sulfur isotope (their $\delta^{34}S$ is higher than approximately +10‰). Another scenario involves the interaction of the magmas with crustal sulfides characterized by a bimodal distribution of $\delta^{34}S$ values: approximately +2.5‰ and higher than +10‰. In the situation when the assumed contaminant is a heterogeneous mixture of sulfur sources of different isotope composition, different

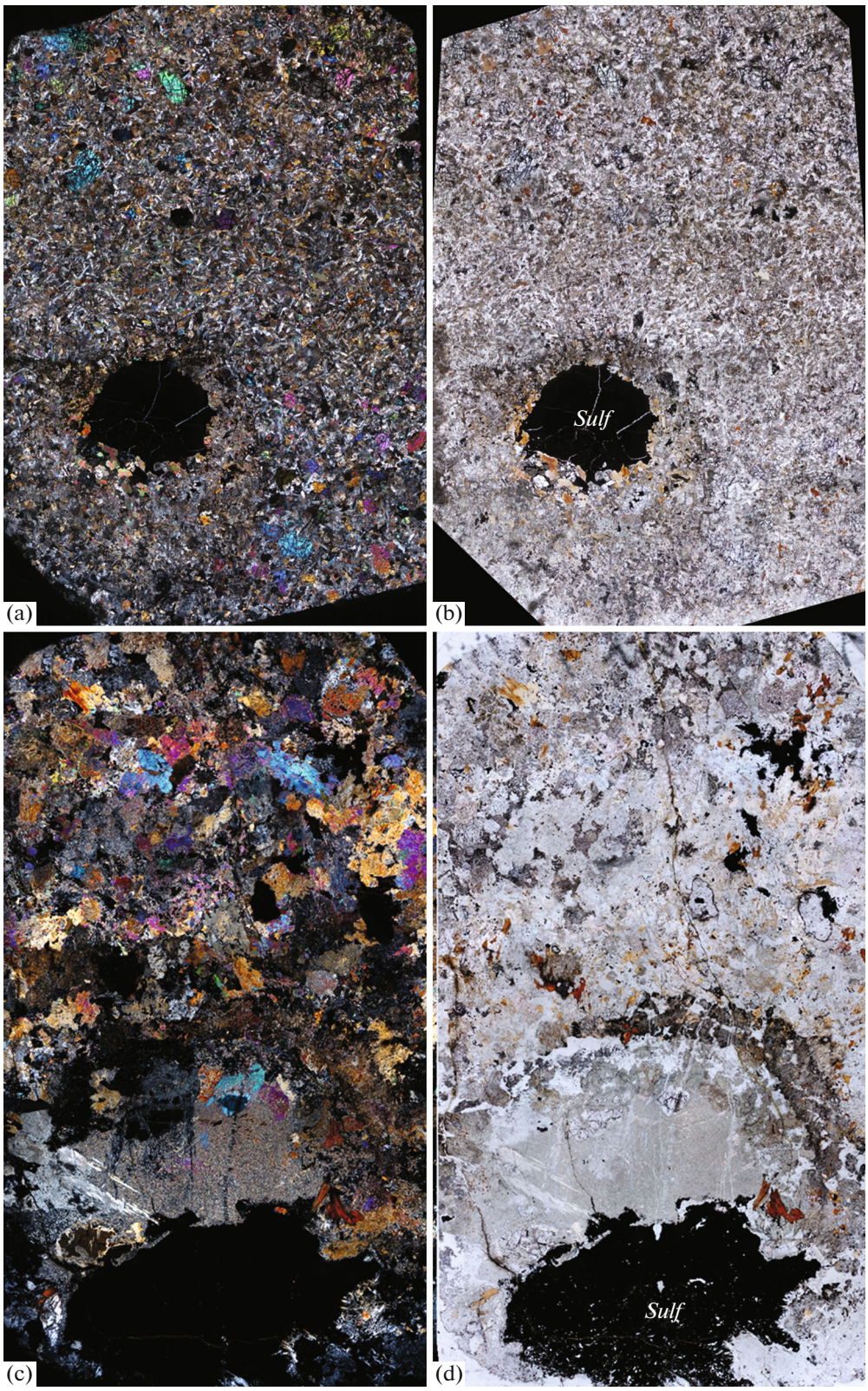

Fig. 4. Panoramic images of thin sections of two rocks with sulfide droplets.
The left-hand photos were taken in plain-polarized light (PPL, crossed polarizers), the right-hand photos are in transmitted light.
(a, b) Picrodolerites, sample 16DV627-1-2, (c, d) mineralized leucogabbro, sample 16DV629-1-2 (Table 1).

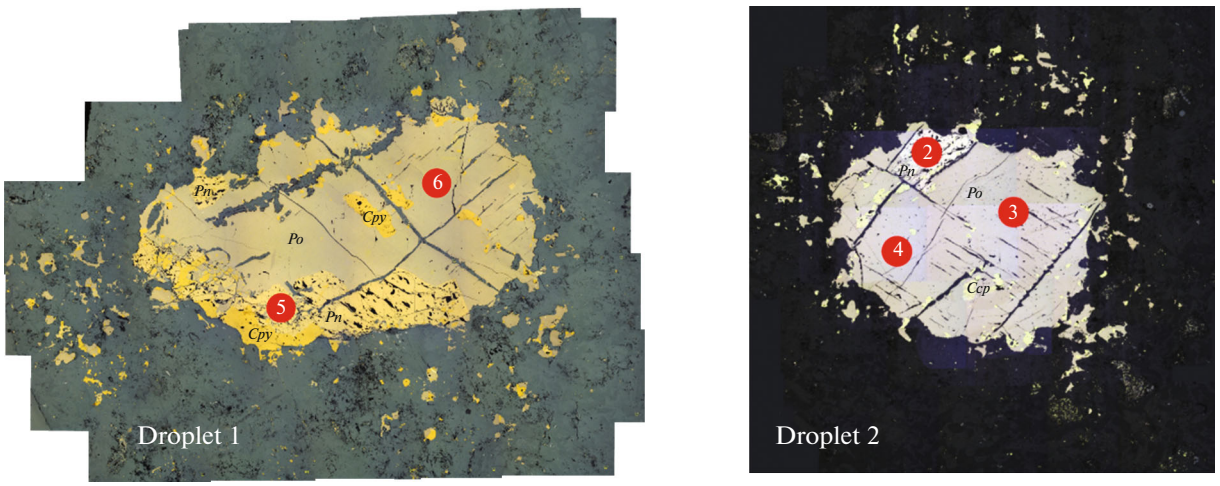

Fig. 5. Microphotograph of two sections of a sulfide droplet from picrodolerite, sample 16DV627-1-2. Numerals show the sites from which microsamples of sulfides were mechanically extracted using a diamond needle.

mixing models with different magma/rock ratios shall be analyzed. To solve this problem, it is necessary to specify more accurately the range of the $\delta^{34}S$ values of the host rocks.

One of the first published values was $\delta^{34}S = +3.2‰$, which was obtained for pyrrhotite from quartz–pyroxene–plagioclase hornfels with abundant disseminated pyrrhotite–chalcopyrite mineralization in the basal zone of the Yoko-Dovyren massif (Vinogradov and Grinenko, 1964). Later on S.A. Gurulev et al. (1978) published a value of $\delta^{34}S = -0.18‰$ for pyrrhotite from a sandy bed in flysch-like sequence of the Ondoko Formation, which underlies the pluton (Konnikov, 1986). Sulfides richer in the ^{34}S isotope were found (Glotov et al., 1998) in the siltstone with pyrite–pyrrhotite veinlets and dolomite with pyrite–sphalerite mineralization: $\delta^{34}S = +7.8‰$ in both instances. The broadest variations in the sulfur isotope composition of sulfides in the host rocks were presented in the dissertation by L.N. Grinenko (1986): data on approximately 30 samples lie within the $\delta^{34}S$ range of $-10‰$ to almost $+27‰$, with a mode of $\delta^{34}S \cong +2‰$, at an average sulfur concentration of 0.54 ± 0.15 wt %. Neither petrographic description of the samples nor their geological settings are presented therein.

We obtained new data on four samples of the host sulfide-bearing rocks (Fig. 6), whose major-component and mineralogical compositions have also been studied (Table 3). The samples of the banded black shales (metasiltstone, samples 07DV104-2 and 07DV105-1) were taken from beneath the central portion of the Yoko-Dovyren massif, at distances of 340 and 300 m from the lower contact (Bolshoi Prospect). The quartz sandstone sample (17DV815-1) was sampled at the northeastern closure of the pluton, at the southern tip of Inyaptuk Lake (Ozernyi Prospect), at a distance of about 500 m of the lower contact. The sample of the poorly mineralized quartz-bearing dolomite (17DV842-1) was taken at the Rybachii Prospect, in the valley of the Ondoko River, approximately 1700 m northwest of the lower contact. The varieties of the sampled rocks characterize the variability of the Late Proterozoic sandy shale rocks of the Ondoko Group with carbonate beds (Konnikov, 1986). The sulfide mineralization of all of these samples is dominated by pyrite (Fig. 6). In spite of the high abundance of sulfides in samples 07DV104-2 and 07DV105-1 (approximately 5.5 and 10%, respectively), we failed to handpick sufficient amounts of the reasonably pure fine-grained fractions. We were thus left with the only possibility of assuming that the $\delta^{34}S$ values of these samples are close to $+8.0‰$, which has been obtained for the pyrite-bearing siltstone (Glotov et al., 1998). We have studied sulfur isotope composition in samples 17DV815-1 and 17DV842-1 (Table 3).

Mass-balance calculations for the mixing of the sulfur sources. The traditional approach to evaluations of the degree of crustal contamination of an orthomagmatic system involves the application of material-balance equations that describe the mixture of two reservoirs (components), which have the following form when applied to sulfur isotope composition (Ripley and Li, 2003):

$$\delta^{34}S_{mixture} = \frac{\delta^{34}S_{con} f_{con} C^{S}_{con} + \delta^{34}S_{mag} f_{mag} C^{S}_{mag}}{f_{con} C^{S}_{con} + f_{mag} C^{S}_{mag}}, \quad (1)$$

where $\delta^{34}S_{con}$ and $\delta^{34}S_{mag}$ are the isotope compositions, f_{con} and $f_{mag} = 1 - f_{con}$ are the mixing proportions, and C^{S}_{con} and C^{S}_{mag} are the sulfur concentrations for the assimilated component (contaminant) and original sulfide magma. The denominator of this expression includes an expression for the bulk sulfur

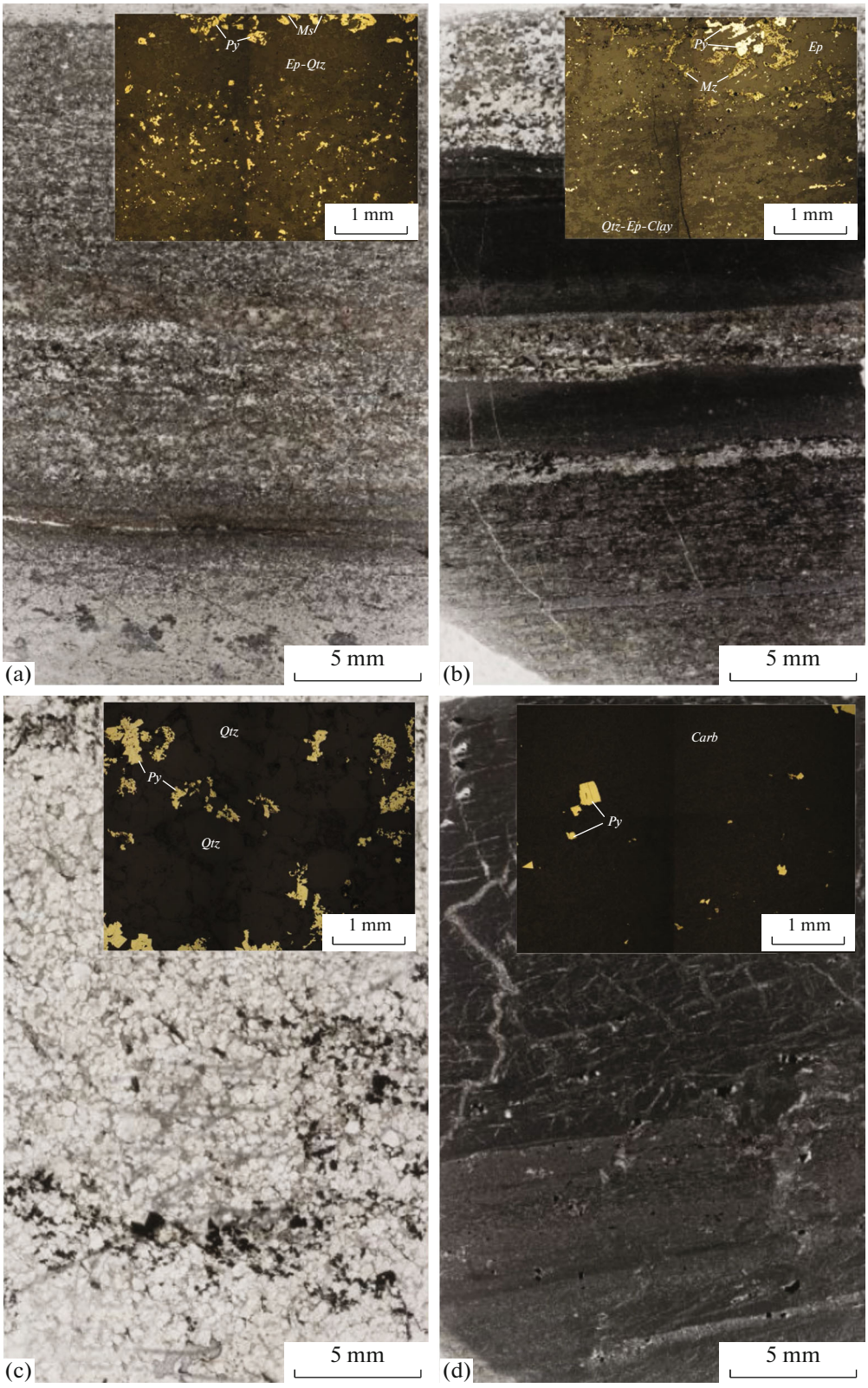

Fig. 6. Microphotographs (in transmitted light) of the studied host rocks with pyrite mineralization (microphotographs in reflected light in the insets). Samples of the banded black shales (metasiltstone): (a) sample 07DV104-2, (b) sample 07DV105-1 (with quartz sandstone beds), (c) quartz sandstone, sample 17DV815-1, (d) pyrite- and quartz-bearing dolomite, sample 17DV842-1.

Table 3. Composition and isotope characteristics of the host rocks

Component	07DV104-2	07DV105-1	17DV815-1	17DV842-1
SiO_2	58.59	57.30	81.92	32.22
TiO_2	0.77	0.69	0.31	0.05
Al_2O_3	14.46	12.89	3.08	1.39
FeO	5.01	5.22	4.90	6.23
MnO	0.08	0.05	0.01	0.35
MgO	2.36	2.41	1.60	9.28
CaO	9.39	10.97	0.24	21.19
Na_2O	1.34	0.70	0.08	<0.05
K_2O	3.55	3.05	0.32	0.30
P_2O_5	0.11	0.08	0.05	0.03
Cr_2O_3	0.012	0.010	0.020	0.002
NiO	0.005	0.004	0.004	
S	1.96	3.08	3.26	0.16
LOI	1.60	2.79	3.58	27.97
Total	99.23	99.24	99.38	99.17
$\delta^{34}S$, ‰	n.d.	n.d.	9.40 ± 0.14 (n = 2)	2.20

concentration in the contaminated system (as the final mixture of the components). An analogous calculation for the concentrations of major and admixture elements in the mixture makes it possible to estimate how realistic are the model values of f_{con} and f_{mag}. This is often ignored, so that discussion of the assimilation effects is reduced solely to the analysis of the isotope (but not chemical) characteristics.

In using Eq. (1), one cannot specify the degree of homogenization of the sulfur isotope ratios in the contaminated system assuming that the mixing products are groups of sulfide clusters with an equally probable distribution of $\delta^{34}S_{mixture}$ over the volume. This problem becomes, however, acute when one tries to interpret data on mineralized rocks and ores that might have been originally formed as a result of earlier accumulation of sulfides with juvenile sulfur characteristics. Hence, mass-balance calculations shall be appended with considerations of the probable mechanisms of isotope homogenization of the mixture, if a homogeneous distribution of sulfur isotope characteristics in grains of the ore minerals is observed (particularly if the contamination proportion is high).

Figure 7 displays calculated mixing lines for the systems ore-bearing magma–contaminant, in which the contaminant is assumed to be a virtual host rock having characteristics of the pyrite-bearing quartzite (sample 17DV815-1) that contains 3.26 wt % relatively isotopically heavy sulfur with $\delta^{34}S_{con}$ = +9.4‰ (Table 3). The simulations were carried out for four samples from apophysis DV10: (1) picrodolerite 16DV627-1 with large sulfide globules and droplets and with average characteristics corresponding to $\delta^{34}S$ = +8.65‰ at 0.22% S in the rock; (2) olivine gabbronorite DV10 with small sulfide droplets ($\delta^{34}S$ = +6.2‰, 0.82% S), (3) mineralized olivine gabbronorite 16DV628-2 ($\delta^{34}S$ = +2.53‰, 3.43% S), and (4) net-textured ore 07DV107-1 ($\delta^{34}S$ = +2.09‰, 9.11% S). With regard to the aforementioned uncertainties, the calculations were of semiquantitative nature, and the possibility of rock contamination with an even heavier sulfur isotope composition was not analyzed at all (see Table 1 for data on samples 16DV627-1-3 and 19DV928-1).

If each of the samples is a result of mixing according to Eq. (1), then the only unknown quantities are the composition of one of the components of the mixture, namely, the composition of the original sulfide magma (including $\delta^{34}S_{mag}$ and sulfur concentration C^S_{mag}) and the proportion of the contaminant f_{con} that shall be added to this sulfide precursor to make the composition of the product matching that of the real ore or rock. The problem is simplified if the isotope composition of the precursor is either known or can be specified: in our situation, we have studied two scenarios, which corresponded to juvenile sulfur with $\delta^{34}S_{mag}$ = 0 (Fig. 7a) and $\delta^{34}S_{mag}$ = +2‰ (Fig. 7b). The solution can then be found analytically, by adding relations for the estimation of the bulk sulfur composition to Eq. (1)

$$S_{mixture} = f_{con}C^S_{con} + f_{mag}C^S_{mag} \text{ and } f_{mag} = 1 - f_{con} \quad (2, 3)$$

or numerically, by selecting optimal values for $\delta^{34}S_{mag}$, C^S_{mag}, and f_{con} from among a series of arbitrary param-

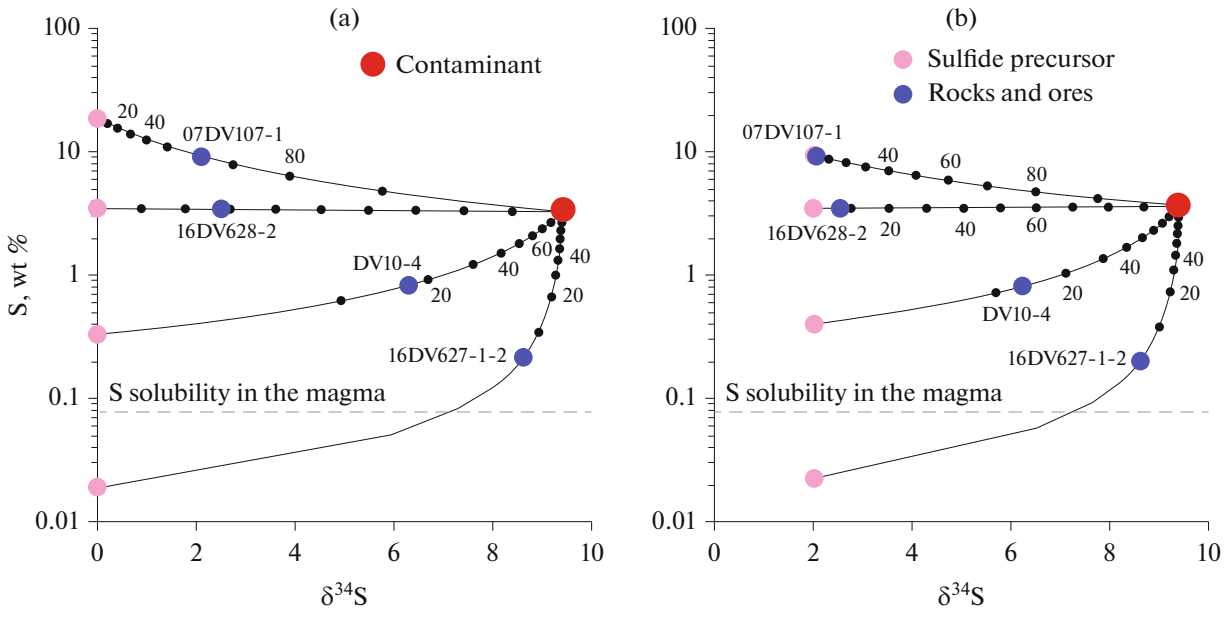

Fig. 7. Calculated lines of contamination of the original sulfide systems (sulfide precursors) with a component with characteristics of the pyrite-bearing quartzite, sample 17DV815-1 (Table 3). Blue circles are the composition of the real sulfide-bearing rocks and ores (Table 1). Numerals near the mixing curve show the proportion of the contaminant. Gray dashed lines show the sulfur solubility in the Dovyren magma (Ariskin et al., 2016).

eters. Figures show data obtained by the latter technique.

In a situation with $\delta^{34}S_{mag} = 0$, the precursor of the high-grade net-textured ore has contained twice higher sulfur concentration than in the ore (18.5 wt % S), which roughly corresponds to 50% sulfides in the original system. This estimate is of virtual nature and shows that an ore with isotope–chemical characteristics of the real ore could be produced if much sulfides had been "preparatorily" accumulated from the main magma volume. For the mineralized olivine gabbronorite (sample 16DV628-2), the virtual sulfur concentration in the precursor practically exactly coincides with that in the probable contaminant. For the rocks with sulfide droplets that contain less than 1 wt % sulfur but possess high $\delta^{34}S_{mag} > +6$, the parental magma should have contained lower (0.33 wt % S for sample DV10) to very low (for sample 16DV627-1) sulfur concentrations. Thus, the solution of this problem for the net-textured ore requires the maximum proportion of contaminant of about 60%. For sample 16DV628-2, approximately 30% assimilated material is required, and the rock samples with sulfide globules (DV10 and 16DV627-1) require 17 and 6%, respectively (Fig. 7a).

The high proportions of contaminant required for the ore samples imply that the hybrid systems should have possessed anomalous petrochemical characteristics, indicating that the shift of the isotope composition $\delta^{34}S_{mag}$ from 0 to approximately +2‰ should have occurred at a much lower concentration of sulfides in the parental magma before their accumulation in the chamber. At the same time, the very low sulfur concentration in the possible precursor of the picrodolerite (sample 16DV627-1, Fig. 7a) sets another signal. Obviously, the fact that this sample contains sulfide droplets indicates that the magma was saturated with the sulfide phase, i.e., sulfur concentration in the magma was no lower than 0.08 wt % (Ariskin et al., 2016) (dashed lines in Fig. 7). If this concentration is assumed as the starting one (and also assuming, again, that $\delta^{34}S_{mar} = 0$), the assimilation of rocks of the same sulfur isotope composition ($\delta^{34}S_{con} = +9.4‰$) suggests that they should have contained about 0.25 wt % sulfur, and the proportion of the contaminant was close to 80%. This puts forth the problem of the anomalously high degree of contamination of the initial magmatic system. Such estimates are in conflict with regular petrochemical trends and geochemical features of the contact rocks of the Dovyren complex, as well as with the results of thermodynamic simulations, which indicate that the variations in the temperature and composition of the parental magmas were generally insignificant (Ariskin et al., 2018b).

Assuming a parental magma with $\delta^{34}S_{mag} = +2$ (which is close to the sulfur isotope composition of ores in apophysis DV10, Table 1), we minimized the excess assimilation for the sulfide-rich rocks (Fig. 7b). This problems remain, however, for the picrodolerite (sample 16DV627-1), if by analogy with what was done previously, we assume that the sulfur concentration in the parental magma corresponds to the sulfur

solubility. The condition $S_{mag} = 0.08$ wt % provides a numerical solution for this sample if the proposed contaminant contains 0.45 wt % S, and the degree of assimilation is close to 70%. We believe that this dilemma can be resolved based on natural geological observations, which indicate that sulfides richest in the ^{34}S isotope are found exactly in the inner-contact zone of the studied apophysis (Fig. 3). This implies that contact processes should have played an important role and could have affected exchange in sulfur isotopes between the magma reservoir and host rocks.

Isotope exchange mediated by a gas phase? According to our data, the parental magmas of the Yoko-Dovyren massif have had temperatures of 1300–1200°C, with the minimum estimates typical of the marginal parts and associated sills/apophyses (Ariskin et al., 2016, 2018b). According to (Kislov, 1998), the thickness of the thermal aureole in the host rocks varies from 100–200 to 400 m, and the outer-contact siltstone is transformed into quartz- and biotite-rich and plagioclase–amphibole–pyroxene hornfels, whose thicknesses reach 3–5 m and are locally as large as 10 m. This contact metamorphism requires large-scale dehydration, with the possibility of the thermal decomposition of sulfides in the sedimentary rocks adjacent to the intrusive contact. E. Ripley was among the first to emphasize the importance of such processes (Ripley, 1981) with reference to the problems of sulfide mineralization at the Dunka Road deposit in the Duluth complex, Minnesota, United States. He suggested that the pyrite may have been decomposed according to the reaction

$$FeS_2 + 3H_2O(\text{vapor}) + 2.5C \rightarrow 2FeS + 1.5CO_2 + CH_4 + 2H_2S, \quad (4)$$

and assumed that the newly formed H_2O-bearing fluid may have interacted with the troctolite magma to produce sulfides with variable sulfur isotope composition. A thermodynamic analysis of a situation when magmatic plutons thermochemically affect graphite- and sulfide-bearing pelites under strongly reducing conditions is presented in (Poulson and Ohmoto, 1989). These authors have determined that the dominant fluid components at low pressures, high temperatures, and relatively low oxygen fugacity are indeed H_2O, CO_2, CH_4, and H_2S. The occurrence of H_2S in the vapor phase at high temperatures suppresses H_2O activity in the fluid and expands the ranges of parameters suitable for the dehydration of sulfide-bearing sedimentary rocks. Later, a set of computations for a broader spectrum of redox conditions and pressures was presented in (Tomkins, 2010), with the computations done using the TERMOCALC and PerpleX softwares.

The generation of H_2S-bearing fluids at the peripheries of the intrusive body thus provides a potential for selective sulfur transfer from the graphite-bearing pelites into the magma chamber and does not require either complete melting or volume assimilation of the host rocks (Poulson and Ohmoto, 1989). This mechanism ideally suites to the geological setting in which the Dovyren complex was formed, including intrusive bodies and apophyses that were emplaced into the carbon-bearing carbonate–terrigenous rocks of the Ondoko Group (Gurulev, 1965; Konnikov, 1986). An indirect argument in support of the plausibility of this transfer is the decrease in the content of organic carbon (up to its complete disappearance) in the terrigenous rocks with decreasing distance from their contact with the intrusion (Kislov, 1998).

The possibility of efficient transfer of sulfur isotopes across a contact zone between two sulfide-bearing reservoirs with different $\delta^{34}S$ values is explained by that the H_2S component of the fluid inherits its sulfur isotope composition from the pyrite that entered decomposition reaction (4). Because of the high temperatures of the irreversible reaction (4), sulfur isotope fractionation between the products of this reaction (pyrrhotite and H_2S) can be viewed as negligibly insignificant. According to the *Po*–H_2S fractionation equation (Li and Liu, 2006) at 1000°C (which is the maximum temperature for which estimates of isotope fractionation were presented by these authors), the sulfur fractionation coefficient in this system is 0.15‰. This estimate is the minimal and corresponds to the maximum temperatures of the contact processes that were associated with the emplacement and crystallization of the Dovyren complex. The maximum estimate, which corresponds to the beginning of volume thermal decomposition of the pyrite (approximately 500°C; Yan et al., 2008), is 0.42‰. The range of these estimates is comparable within the accuracy of sulfur isotope analysis. Hence, the value of $\delta^{34}S$ of the hydrogen sulfide generated at thermal decomposition of the pyrite should have been close to that of the original pyrite.

The interaction of H_2S-bearing fluid with the bivalent iron of sulfide-saturated magmatic melt can be represented by the reaction

$$H_2S + FeO(\text{magma}) \rightarrow FeS\downarrow + H_2O, \quad (5)$$

which results in sulfides whose sulfur isotope composition was inherited from the parental magma and modified by that of the decomposed sulfides of the host rocks. This mechanism is able to explain the occurrence of picrodolerite with high $\delta^{34}S$ values of their sulfides and low sulfur concentrations at contacts with the apophyses, as well as the absence (or insignificant values) of contamination signals in the olivine cumulates upward from the intrusive contact. Moreover, reaction (4) implies that sulfur can be extracted from some volume of the host rocks into a single fluid phase to homogenize the sulfur isotope parameters of sulfur extracted from the host rocks before reaction (5) began. This helps in conciliating inconsistencies

emerging when the mechanism of simple additive contamination is analyzed.

The scenario presented above requires iron extraction from the magmatic melt in a weight proportion that is roughly twice larger than the introduced sulfur amount. For the picrodolerite (sample 16DV627-1) that contains ~0.2 wt % sulfur (Table 1), this is equivalent to roughly 0.5% FeO depletion in the melt. These relations eliminate the problem of the volume assimilation of sedimentary rocks for producing the sulfide droplets enriched in the heavy ^{34}S sulfur isotope. Hence, a factor that resulted in a significantly heavier sulfur isotope composition in the basal zone of apophysis DV10 at magmatic temperatures could have been interaction of the melt with H_2S-bearing fluid of, in fact, metamorphic nature (Tomkins, 2010). If H_2S was extracted for a long enough time from a large volume of sediments or sedimentary rocks, as well as at lower interaction temperatures, the sulfur isotope composition of the sulfide material may have been additionally shifted by no more than 0.5–1‰.

Experimental evidence. Not long ago, results of experiments that studied the partial melting of black shales (pelites) of the Virginia Formation were published. The rocks were sampled outside the thermal aureole of the Duluth complex, in the host rocks (Virtanen et al., 2020). The experiments were conducted under a pressure of 2 kbar and at temperatures of 700–1000°C. These experiments have demonstrated that hydrosilicates are dehydrated at 700°C with the release of most of the sulfur and carbon of the black shales into the fluid phase. At 1000°C, the original sulfides are transformed into droplets of Cu- and Ni-bearing pyrrhotite. This interesting observation confirms the efficiency of contact-metamorphic processes based on reaction (4).

CONCLUSIONS

(1) High-precision analysis for sulfur isotope composition with the application of methods of local mechanical hand-picking of sulfide fractions was conducted for ten plagioperidotite samples, which represented the stratigraphic section of a thick (about 300 m) swell of a mineralized apophysis of the Yoko-Dovyren massif in the northern Baikal area. The $\delta^{34}S$ values were determined to broadly vary from +11 to −1.9‰, with sulfides maximally enriched in isotopically heavy sulfur found in ~10-m horizon near the lower contact of the apophysis and minimally enriched sulfides occurring near the upper contact.

(2) Sulfide droplets from picrodolerite from the immediate vicinity of the lower contact of the apophysis (Pshenitsyn et al., 2020) show a narrow range of $\delta^{34}S = +8.65 \pm 0.34$‰ ($n = 5$). The high-grade net-textured ores, mineralized olivine gabbronorite, and a mineralized leucogabbro dike are characterized by little varying values of $\delta^{34}S = +2.09$ to +2.53‰.

(3) The composition of four samples of the host carbonate–terrigenous rocks was analyzed by XRF. The rocks contain relatively much sulfur (up to 3–3.5 wt %), which corresponds to about 10% sulfides. A sample of the pyrite-bearing quartzite (17DV815-1) was determined to have $\delta^{34}S = +9.40 \pm 0.14$‰, and the pyrite-bearing dolomite yielded $\delta^{34}S = +2.20$‰.

(4) Simple scenarios of additive mixing of isotopically contrasting reservoirs, which correspond to a juvenile magmatic source ($\delta^{34}S = 0$ and +2‰), and pyrite with isotopically heavy sulfur ($\delta^{34}S = +9.4$‰) are demonstrated to require high degrees of assimilation of the host rocks (as much as 60–80%) and need isotopic equilibration of the hybrid system. In the situation with the contact picrodolerite with sulfide globules, such mechanism is inconsistent with the estimated solubility of sulfide sulfur in the Yoko-Dovyren magma, which is close to 0.08 wt % (Ariskin et al., 2016).

(5) The high $\delta^{34}S$ values in the basal rocks of the plagioperidotite apophysis are explained by an alternative mechanism of the contamination of the sulfide-saturated magma based on the thermal decomposition of pyrite from the host rocks. This process was associated with the formation of contact-metamorphic H_2S-bearing fluid (Poulson and Ohmoto, 1989), which interacted with the magmatic melt at the peripheries of the intrusive body and produced minor amounts of sulfides with elevated and high $\delta^{34}S$ values. This scenario does not require volume assimilation of the host rocks and is consistent with petrologic and geochemical characteristics of the magmas and cumulates.

ACKNOWLEDGMENTS

The authors thank G.S. Nikolaev (Vernadsky Institute of Geochemistry and Analytical Chemistry, Russian Academy of Sciences) for help in the course of the fieldwork and consultations concerning the presented materials. The physicochemical interpretation of the results was largely stimulated during their discussion with V.B. Polyakov (Korzhinskii Institute of Experimental Mineralogy, Russian Academy of Sciences). Special thanks are due to M.A. Yudovskaya (Institute of Geology of Ore Deposits, Petrography, Mineralogy, and Geochemistry, Russian Academy of Sciences) and A.S. Mekhonoshin (Vinogradov Institute of Geochemistry, Siberian Branch, Russian Academy of Sciences) for valuable comments on the manuscript.

FUNDING

This paper presents results obtained in the course of studies under projects nos. 16-17-10129 and 18-17-00126 of the Russian Science Foundation. Material for the separation of sulfide fractions and mineralogical studies was prepared under a government-financed research project for the Vernadsky Institute of Geochemistry and Analytical Chemistry, Russian Academy of Sciences. The composition of

mineral phases was analyzed at the Laboratory for Analytical Techniques of High Spatial Resolution at the Department of Petrology, Moscow State University (analysts V.O. Yapaskurt and N.N. Korotaeva).

REFERENCES

Ariskin, A.A., Konnikov, E.G., Danyushevskii, L.V., et al., Geochronology of the Dovyren intrusive complex, northwestern Baikal Area, Russia, in the Neoproterozoic, *Geochem. Int.,* 2013, vol. 51, no. 11, pp. 859–875.

Ariskin, A.A., Danyushevsky, L.V., Bychkov, K.A., et al., Modeling solubility of Fe–Ni sulfides in basaltic magmas: the effect of Ni in the melt, *Econ. Geol.,* 2013, vol. 108, no. 8, pp. 1983–2003.

Ariskin, A.A., Kislov, E.V., Danyushevsky, L.V., et al., Cu–Ni–PGE fertility of the Yoko-Dovyren layered massif (northern Transbaikalia, Russia): thermodynamic modeling of sulfide compositions in low mineralized dunites based on quantitative sulfide mineralogy, *Mineral. Deposita,* 2016, vol. 51, pp. 993–1011.

Ariskin, A.A., Bychkov, K.A., Nikolaev, G.S., and Barmina, G.S., The COMAGMAT-5: modeling the effect of Fe–Ni sulfide immiscibility in crystallizing magmas and cumulates, *J. Petrol.,* 2018a, vol. 59, no. 2, pp. 283–298.

Ariskin, A., Danyushevsky, L., Nikolaev, G., et al., The Dovyren intrusive complex (southern Siberia, Russia): insights into dynamics of an open magma chamber with implications for parental magma origin, composition, and Cu–Ni–PGE fertility, *Lithos,* 2018b, vol. 302–303, pp. 242–262.

Ariskin, A.A., Nikolaev, G.S., Danyushevsky, L.V., et al., Genetic interpretation of the distribution of PGE and chalcogens in sulfide–mineralized rocks from the Yoko-Dovyren layered intrusion, *Geochem. Int.,* 2018c, vol. 56, no. 13, pp. 1322–1340.

Ariskin, A.A., Nikolaev, G.S., Danyushevsky, L.V., et al., Geochemical evidence for the fractionation of iridium group elements at the early stages of crystallization of the Dovyren magmas (northern Baikal area, Russia), *Russ. Geol. Geophys.,* 2018d, vol. 59, no. 5, pp. 459–471.

Ariskin, A.A., Danyushevsky, L.V., Fiorentini, M.L., et al., Petrology, geochemistry, and the origin of sulfide-bearing and PGE-mineralized troctolites from the Konnikov Zone in the Yoko–Dovyren layered Intrusion, *Russ. Geol. Geophys.,* 2020, vol. 61, no. 5–6, pp. 611–633.

Baburin, L.M., *Geologicheskoe stroenie i metallonosnost' Dovyrenskogo bazit–giperbazitovogo massiva. Okonchatel'nyi otchet o rezul'tatakh poiskovo–razvedochnykh rabot Baikal'skoi kompleksnoi partii za 1960–1963 gg.* (Geological Structure and Metal Potential of the Dovyren Basic–Ultrabasic Massif. Final Report on Results of Prospecting Works of the Baikal Complex Party for 1960–1963), Ulan–Ude: Buryatskoe geologicheskoe upravlenie, 1964.

Baker, D.R. and Moretti, R., Modeling the solubility of sulfur in magmas: a 50-year old geochemical challenge, *Rev. Mineral. Geochem.,* 2011, vol. 73, pp. 167–213.

Barnes, S.J., Cruden, A.R., Arndt, N., and Saumur, B.M., The mineral system approach applied to magmatic Ni–Cu–PGE sulphide deposits, *Ore Geol. Rev.,* 2016, vol. 76, pp. 296–316.

Chung, H.-Y. and Mungall, J.E., Physical constraints on the migration of immiscible fluids through partially molten silicates, with special reference to magmatic sulfide ores, *Earth Planet. Sci. Lett.,* 2009, vol. 286, pp. 14–22.

Distler V.V. and Stepin, A.G., Low-sulfide platinum-bearing horizon of the Yoko-Dovyren layered ultrabasic–basic intrusion (Northern Baikal region), *Dokl. Ross. Akad. Nauk,* 1993, vol. 328, no. 4, pp. 498–501.

Ernst, R.E., Hamilton, M.A., Soderlund, U., et al., Long-lived connection between southern Siberia and northern Laurentia in the Proterozoic, *Nature Geosci.,* 2016, vol. 9, pp. 464–469.

Fortin, M.–A., Riddle, J., Desjardins-Langlais, Y., and Baker, D.R., The effect of water on the sulfur concentration at sulfide saturation (scss) in natural melts, *Geochim. Cosmochim. Acta,* 2015, vol. 160, pp. 100–116.

Glotov, A.I., Kislov, E.V., Orsoev, D.A., et al., Sulfur isotope geochemistry in different types of the sulfide mineralization of the Yoko-Dovyren massif (northern Baikal region), *Geol. Geofiz.,* 1998, vol. 39, no. 2, pp. 228–233.

Grinenko, L.N., Sulfur sources of basic-ultrabasic rocks and related sulfide copper–nickel ores, *Doctoral (Geol.-Min.) Dissertation,* Moscow: GEOKhI RAN, 1986.

Gurulev, S.A., *Geologiya i usloviya formirovaniya Ioko-Dovyrenskogo gabbro–peridotitovogo massiva* (Geology and Conditions of Formation of the Yoko–Dovyren gabbro–peridotite massif), Moscow: Nauka, 1965.

Gurulev, S.A., Truneva, M.F., Kaviladze, M.Sh., and Melashvili, T.A., *Sulfur isotope composition of copper–nickel deposits of Nortehrn Baikal region in relation with magmatic replacement, Kontaktovye protsessy i orudenenie v gabbro–peridotitovykh intruziyakh* (Contact Processes and Mineralization in the Gabbro–Peridotite Intrusions), Moscow: Nauka, 1978, pp. 125–135.

Izrailevich, I.S., Kalashnikov, V.A., Zalesov, Yu.N., and Bazhin, A.F., From history of mass-specctrometric laboratory of TsZL UEKhK, *Analitika i kontrol',* 2003, vol. 7, no. 4, pp. 316–318.

Kacharovskaya, L.N., Konnikov, E.G., and Kaviladze, M.Sh., Sulfur isotope composition and genesis of sulfide ores of the Yoko-Dovyren basic–ultrabasic massif, *Geol. Geofiz.,* 1986, no. 5. C. 52–57.

Karykowski, B.T., Maier, W.D., Groshev, N.Y., et al., Critical controls on the formation of contact-style PGE–Ni–Cu mineralization: evidence from the Paleoproterozoic Monchegorsk Complex, Kola region, Russia, *Econ. Geol.*, 2018, vol. 113, pp. 911–935.

Kiseeva, E.S. and Wood, B.J., The effects of composition and temperature on chalcophile and lithophile element partitioning into magmatic sulphides, *Earth Planet. Sci. Lett.,* 2015, vol. 424, pp. 280–294.

Kislov, E.V., *Ioko-Dovyrenskii rassloennyi massiv* (Yoko–Dovyren Layered Massif), Ulan-Ude: Izd. BNTs, 1998.

Kislov, E.V. and Khudyakova, L.I., Yoko-Dovyren layered massif: composition, mineralization, overburden and dump rock utilization, *Minerals,* 2020, vol. 10, p. 682. https://doi.org/10.3390/min10080682

Konnikov, E.G., *Differentsirovannye giperbazit–bazitovye kompleksy dokembriya Zabaikal'ya* (Precambrian Differentiated Ultrabasic–Basic Complexes of Transbaikalia), Novosibirsk: Nauka, 1986. 127 s.

Korost, D.V., Ariskin, A.A., Pshenitsyn, I.V., and Khomyak, A.N., X-Ray computed tomography as a method for reproducing 3D characteristics of sulfides and spinel disseminated in plagiodunites from the Yoko-Dovyren Intrusion, *Petrology,* 2019, vol. 27, no. 4, pp. 370–385.

Krivolutskaya, N.A., *Siberian Traps and Pt–Cu–Ni Deposits in the Noril'sk Area,* Cham–Heidelberg–New York–Dordrecht–London: Springer, 2016.

Li, Y.B. and Liu, J.M., Calculation of sulfur isotope fractionation in sulfides, *Geochim. Cosmochim. Acta,* 2006, vol. 70, pp. 1789–1795.

Li, C. and Ripley, E.M., Sulfur contents at sulfide–liquid or anhydrite saturation in silicate melts: empirical equations and example applications, *Econ. Geol.,* 2009, vol. 104, pp. 405–412.

Likhachev, A.P., *Platino-medno-nikelevye i platinovye mestorozhdeniya* (Platinum-Copper-Nickel and Platnum Deposits), Moscow: Eslan, 2006.

Maier, W.D., Why are there no major Ni–Cu sulfide deposits in large layered mafic–ultramafic intrusions?, *Can. Mineral.,* 2001, vol. 39, pp. 547–556.

Maier, W.D., Platinum-group element (PGE) deposits and occurrences: mineralization styles, genetic concepts, and exploration criteria, *J. Afr. Earth Sci.,* 2005, vol. 41, pp. 165–191.

Maier, W.D. and Groves, D.I., Temporal and spatial controls on the formation of magmatic PGE and Ni–Cu deposits, *Mineral. Deposita,* 2011, vol. 46, pp. 841–857.

Manuilova, M.M. and V.V. Zarubin *Vulkanogennye porody dokembriya Severnogo Pribaikal'ya* (Precambrian Volcanogenic Rocks of the Northern Baikal Region), Leningrad: Nauka, 1981.

Mao, Y–J., Barnes, S.J., Duan, J., et al., Morphology and particle size distribution of olivines and sulphides in the Jinchuan Ni–Cu sulphide deposit: evidence for sulphide percolation in a crystal mush, *J. Petrol.,* 2018, vol. 59, no. 9, pp. 1701–1730.

Naldrett, A.J., *Magmatic Sulfide Deposits: Geology, Feochemistry and Exploration,* Heidelberg, Berlin: Springer–Verlag, 2004.

Naldrett, A.J., *Fundamentals of magmatic sulfide deposits, Magmatic Ni–Cu and PGE Deposits: Geology, Geochemistry and Genesis, Rev Econ. Geol.,* C. Li and E.M. Ripley, Eds., Denver: Soc. Econom. Geol, 2011, vol. 17, pp. 1–50.

Orsoev, D.A., Mekhonoshin, A.S., Kanakin, S.V., et al., Gabbro–peridotite sills of the Late Riphean Dovyren plutonic complex (northern Baikal area, Russia), *Russ. Geol. Geophys.,* 2018, vol. 59, no. 5, pp. 472–485.

Poulson, S.R. and Ohmoto, H., Devolatilization equilibria in graphite–pyrite–pyrrhotite bearing pelites with application to magma–pelite interaction, *Contrib. Mineral. Petrol.,* 1989, vol. 101, pp. 418–425.

Pshenitsyn I.V., Ariskin A.A., Nikolaev G.S., et al., Morphology, mineralogy, and composition of sulfide droplets in picrodolerite from a near-bottom apophysis of the Yoko-Dovyren layered intrusion, *Petrology,* 2020, vol. 28, no. 3, pp. 280–297.

Pshenitsyn, I.V., Ariskin, A.A., Nikolaev, G.S., et al., Protosulfide melts in the ore-bearing gabbroperidotite sills of the Yoko-Dovyren intrusion, *Geochem. Int.,* 2022. (in press).

Rad'ko, V.A., Model of dynamic differentiation of intrusive traps of the Siberian Platform, *Geol. Geofiz.,* 1991, no. 11, pp. 19–27.

Rad'ko, V.A., *Fatsii intruzivnogo i effuzivnogo magmatizma Noril'skogo raiona* (Facies of the Intrusive and Effusive Magmatism of the Norilsk Region), St. Petersburg: FGBU "VSEGEI", 2016.

Ripley, E.M., Sulfur isotopic studies of the Dunka road Cu–Ni deposit, Duluth complex, Minnesota, *Econ. Geol.,* 1981, vol. 76, pp. 610–620.

Ripley, E.M. and Li, C., Sulfur isotope exchange and metal enrichment in the formation of magmatic Cu–Ni–PGE deposits, *Econ. Geol.,* 2003, vol. 98, pp. 635–641.

Ripley, E.M. and Li, C., Sulfide saturation in mafic magmas: is external sulfur required for magmatic Ni–Cu–PGE ore genesis?, *Econ. Geol.,* 2013, vol. 108, pp. 45–58.

Robertson, J.C., Barnes, J.S., Le Vaillant, M., Dynamics of magmatic sulphide droplets during transport in silicate melts and implications for magmatic sulphide ore formation, *J. Petrol.,* 2016, vol. 56, pp. 2445–2472.

Rytsk, E.Yu., Shalaev, V.S., Rizvanova, N.G., et al., The Olokit Zone of the Baikal Fold Region: new isotope-geochronological and petrogeochemical data, *Geotectonics,* 2002, vol. 36, no. 1, pp. 24–35.

Song, X., Wang, Y., and Chen, L., Magmatic Ni–Cu–PGE deposits in magma plumbing systems: features, formation and exploration, *Geosci. Front.,* 2011, vol. 2, no. 3, pp. 375–384.

Tomkins, A.G., Windows of metamorphic sulfur liberation in the crust: implications for gold deposit genesis, *Geochim. Cosmochim. Acta,* 2010, vol. 74, pp. 3246–3259.

Turutanov, E.Kh., Stepanenko, A.V., and Buyantogtokh, B., 3D model of the Yoko–Dovyren gabbro–peridotite massif (northern Baikal area): gravimetry data, *Vestn. Irk. Gos. Univ.,* 2013, no. 2(73), pp. 88–95.

Vinogradov, A.P. and Grinenko, L.N., On the influence of host rocks on the sulfur isotope composition of sulfides, *Geokhimiya,* 1964, no. 2, pp. 491–499.

Virtanen, V.J., Heinonen, J.S., Molnar, F., et al., Black shale partial melting experiments provide insight into S, C, and Cu assimilation processes in Duluth complex, Minnesota, *Abstract of 14th International Ni—Cu—PGE Symposium and Memorial to Prof. A.J. Naldrett,* 2020, p. 42.

Wang, Z., Jin, Z., Mungall, J.E., and Xiao, X., Transport of coexisting ni–cu sulfide liquid and silicate melt in partially molten peridotite, *Earth Planet. Sci. Lett.,* 2020, vol. 536, p. 116162.

Yan, J., Long Xu, L., and Yang, J., A study on the thermal decomposition of coal-derived pyrite, *J. Analyt. Appl. Pyrol.,* 2008, vol. 82, pp. 229–234.

Yao, Z. and Mungall, J.E., Linking the Siberian flood basalts and giant Ni–Cu–PGE sulfide deposits at Norilsk, *JGR Solid Earth Res.,* 2021.
https://doi.org/10.1029/2020JB020823

Translated by E. Kurdyukov